Low-order modeling for unsteady separated compressible flows by POD-Galerkin approach

Rémi BOURGUET[1], **Marianna BRAZA, Gilles HARRAN**

Institut de Mécanique des Fluides de Toulouse, UMR 5502 CNRS-INPT/UPS,
Allée du Prof. Camille Soula, 31400 Toulouse, France
[1] *Remi.Bourguet@imft.fr*

Alain DERVIEUX

Institut National de Recherche en Informatique et en Automatique,
B.P. 93, 06902 Sophia-Antipolis, France

Abstract. A low-dimensional model is developed on the basis of the unsteady compressible Navier-Stokes equations by means of POD-Galerkin methodology in the perspective of physical analysis and computational savings. This approach consists in projecting the complex physical model onto a subspace determined to reach an optimal statistical content conservation. This leads to a drastic reduction of the number of degrees of freedom while preserving the main flow dynamics. The high-order system formulation is modified and an inner product which couples the contributions of both kinematic and thermodynamic state variables is selected. The associated reduced order model is a quadratic polynomial ordinary differential equation system which presents an inherent sensitivity to POD basis truncation for long-term prediction. A calibration process based on the minimisation of the prediction error with respect to reference dynamics is implemented. The predictive capacities of the low-order approach are evaluated by comparison with results issued from the 2D Navier-Stokes simulation of a transonic flow around a NACA0012 airfoil, at zero angle of incidence. This configuration is characterised by a complex unsteadiness caused by a von Kármán instability mode induced by shock/vortex interaction, and a low frequency buffeting mode.

Key words: Low-order modeling, POD-Galerkin approach, Navier-Stokes equations, compressibility effects.

1. Introduction

The purpose of the present study is to develop a Reduced-Order Model (ROM) for the prediction of the complex wall-flow features induced by compressibilily effects at high transonic regimes. From a general point of view, the objective of surrogate modeling is to mimic a realistic and complex physical model by a *local but faithfull* approximation involving lower calculation costs. In the context of mutli-disciplinary optimisation or fluid/structure interaction, where complex physical simulations are integrated into iterative processes, low-dimensional models can allow drastic gains of computational ressources. Moreover, such approaches represent relevant tools for physical investigations owing to their inherent mathematical simplicity, especially in the transitional case.

To elaborate reduced-order models, meta-modeling like polynomial interpolations, neural networks or response surfaces are often developed on the basis of a pure data-driven approach which involves many high-order computations. The physic-driven methodology presented in this paper consists in a Galerkin projection of the complex model onto a finite-dimensional basis determined to reach optimal energy reconstruction. The physical model is the compressible Navier-Stokes system. The basis is issued from a separable Proper Orthogonal Decomposition (POD, [1], also known as Karhunen-Loève expansion [2]) of the flow variables, which extracts the main fluid energetic properties ([3], among others). The corresponding low-order model is an ordinary differential equation system of considerably reduced dimension compared to the high-order one. This ROM enables the prediction of the main flow dynamics.

Various low-order dynamical models were derived from the incompressible Navier-Stokes system. In 2D, the laminar flow past a circular cylinder [4] and transitional cavity flows [5] were efficiently predicted by POD-Galerkin approach. The relevance of this methodolody was illustrated in the 3D laminar case [6][7] with databases issued from Direct Numerical Simulations. The inherent instability of POD-Galerkin systems was studied and calibration processes lead to significant improvments, based on the addition of an artificial dissipation [8], on data-driven optimisations in the laminar case [9], in the transitional/turbulent case [10], and on the introduction of additional instability or "shift" modes in the low-order basis [11]. POD-Galerkin models were integrated into optimal control processes [12] and error estimates were obtained in this context [13]. Theoretical extensions were developed to increase the robustness of the empirical basis with respect to changes in flow configuration [14]-[17] and to adapt the POD basis to domain deformations [18] in the perspective of design optimisation. The case of reacting flows involving dilatation effects was investigated in [19] by means of a coupling between POD modes, "shift" and "expansion" modes.

For compressible flows, the coupling of kinematic and thermodynamic variables in the state system induces specific difficulties concerning the state variable formulation and the inner product invovled in the POD. In [20] a general framework was provided to derive low-order models based on the inviscid Euler equations, via POD-Galerkin approach, among others. Promising results are reported in [21], considering an approximation of the compressible Navier-Stokes system valid for moderate Mach numbers and cold flows, by means of an isentropic inner product. As discussed in the present paper, a specific variable change considerably simplifies the ODE system obtained after projection of the complex physical model onto the empirical basis [22][23]. Investigations of stability properties lead to relevant ROM for moderate Mach numbers and short time predictions, in laminar and transitional cases [24].

In the present paper, an accurate POD-Galerkin model is derived from the compressible Navier-Stokes system expressed in term of modified state variables. The classical spatial inner product is extended to the compressible case and the corresponding quadratic polynomial ODE system enables flow dynamic reconstructions including all state variable contributions. Taking into account of the inherent instability of this low-order model, a stabilisation strategy is applied. Optimal constant and linear terms are added to the dynamical system in order to minimize a specific prediction error with respect to the initial reference dataset. The reliability of the calibrated low-order model is examined in the high transonic regime, in the two-

dimensional case at first. The unsteady compressible flow past a NACA0012 airfoil at moderate Reynolds number is considered. The database is issued from a direct numerical simulation via ICARE/IMFT compressible solver [25]. The complex unsteadiness of this configuration is induced by compressibility effects and especially by shock/vortex interaction, as detailled in the first section. In the following, the extraction of the empirical POD basis, the development of the Navier-Stokes ROM and the calibration process are described. The predictive capacities of the present low-order approach are quantified in the last section.

2. Physical context

2.1. Transition features in the compressible flow past an airfoil

The transonic flow past a NACA0012 airfoil at zero angle of incidence develops an inherent unsteadiness due to compressible effects during the transition to turbulence. At moderate Reynolds number $0.5 - 1 \times 10^4$, the flow is steady at the incompressible regime. At Mach number higher or equal to 0.3 the onset of a von Kármán instability occurs in the wake (mode I). In the Mach number interval $[0.5, 0.7]$, this mode I becomes more pronounced and the periodic alternating vortex pattern is clearly developed. The near-region is progressively contaminated by the instability developing in the wake. At Mach number 0.75 a lower frequency mode induced by the oscillation of the supersonic pockets is observed (buffeting) and this mode II has disappeared at Mach number 0.85. Thus, the configuration studied in the present paper (Mach number 0.80, Reynolds number 10^4) is characterized by a complex unsteadiness caused by the two instability mode interaction (Fig. 1). More details about the flow physics of this specific two-dimensional configuration can be found in [25][26]-[28].

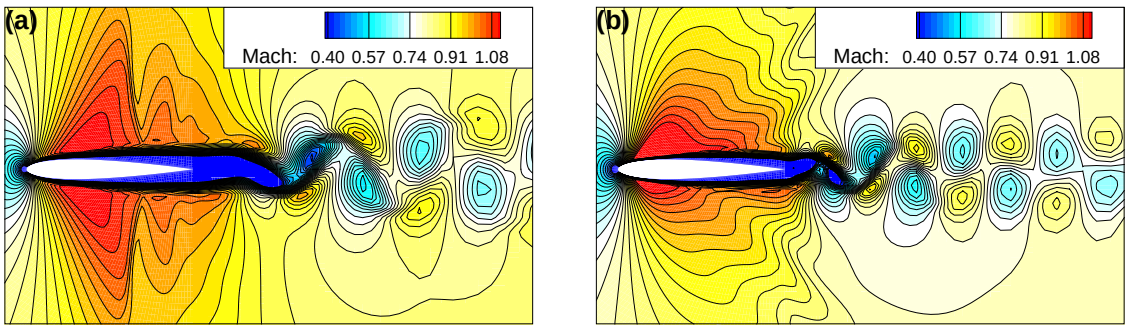

Figure 1. (a) $R_e = 5000$ and $M = 0.85$: Mode I. (b) $R_e = 10,000$ and $M = 0.8$: Mode I and Mode II (present study).

2.2. The compressible Navier-Stokes system

The high-order model to approximate is the unsteady compressible Navier-Stokes system. If no external effort and no external heat flux are imposed on the fluid flow, the governing equations expressed in term of conservative variables can be

formulated as follows, in two dimensions:

$$U_{,t} + F_{i,i} = F_{i,i}^{vis} \quad \text{with} \quad U = \begin{bmatrix} \rho \\ \rho u_1 \\ \rho u_2 \\ \rho e \end{bmatrix}, \; F_i = \begin{bmatrix} \rho u_i \\ \rho u_i u_1 + p\delta_{1i} \\ \rho u_i u_2 + p\delta_{2i} \\ \rho u_i e + p u_i \end{bmatrix}, \; F_i^{vis} = \begin{bmatrix} 0 \\ \tau_{1i} \\ \tau_{2i} \\ \tau_{ij} u_j - q_i \end{bmatrix},$$

where ρ is the volumic mass, u_i are the components of the velocity, p is the thermodynamic pressure which satisfies the ideal gas law $p = \rho R T_p$ where T_p is the temperature and R is the ideal gas constant. $\tau_{ij} = \mu\left((u_{i,j} + u_{j,i}) - 2/3 u_{k,k}\delta_{ij}\right)$ is the viscous effort tensor where μ is the fluid viscosity, q_i are the components of the heat flux ($q_i = -C_T T_{p,i}$, with the conductivity coefficient C_T) and δ_{ij} is Kronecker symbol. e is the total energy defined by:

$$e = C_v T_p + \frac{u_1^2 + u_2^2}{2},$$

where C_v is the specific heat coefficient. $.,t$ and $.,i$ denotes respectively the time and space derivatives. Concerning the boundary conditions at the frontiers of the physical domain, only time-independent relations are prescribed: constant values on inflow frontier and free-stream conditions on the outlet. No-slip condition is imposed on the airfoil.
The numerical dataset is issued from a calculation via ICARE/IMFT compressible solver. This is a structured finite volume code in which Roe's upwind spatial scheme is implemented with MUSCL approach for the convective part and a centered second order scheme for the diffusive term. The temporal integration is ensured by an explicit four-stage Runge-Kutta scheme of fourth order accuracy. The C-type meshgrid ($N_x = 369 \times 89$ nodes) used was validated in the present flow configuration, the corresponding pressure and aerodynamic coefficients are reported in [25].

3. The POD-Galerkin model

3.1. Reduced order basis extraction via POD

The Proper Orthogonal Decomposition is a Singular Value Decomposition which consists in expanding each physical variable as a linear combination of specific eigenfonctions. The POD of a time/space-dependent function v can be written as follows:

$$v(x,t) \approx \sum_{i=1}^{N_{POD}} a_i \Phi_i(x,t), \quad \text{or} \quad v(x,t) \approx \sum_{i=1}^{N_{POD}} y_i(t)\Phi_i(x) \tag{1}$$

assuming time/space separation. y_i are time-dependent functions and Φ_i stationnary spatial modes determined as successive solutions of the following constrained optimisation problem:

$$\Phi_{i+1}(x) = \arg \max_{\phi \in L^2(\Omega)} \left\langle (v - \Pi_i v, \phi)^2 \right\rangle \quad \text{subject to} \quad \|\phi\|^2 = 1, \tag{2}$$

where $< . >$ represents a temporal averaging, Ω is the spatial domain, $(.,.)$ is an inner product which has to be defined on $L^2(\Omega)$ and Π_i is the projector onto $\{\Phi_1, ..., \Phi_i\}$.

Finding Φ_i in (2) is equivalent to find the orthonormalised eigenvectors of a state variable spatial correlation matrix. After discretisation, N_x is the number of space discretisation points and N_t the number of flow snapshots collected. If the first N_{POD} spatial modes are taken into account with $N_{POD} << N_x$ and $N_{POD} << N_t$, the expression (1) provides a low-order approximation of v which is optimal in the sense of energy reconstruction. The "snapshot-POD" technic [29] consists in finding the eigenvectors of the temporal correlation matrix which reduces considerably the size of the problem in the case of numerical simulations where $N_x >> N_t$. The spatial inner product involved in (2) is a crucial point in case of multiple state variables ($v^i, \quad i = 1, ..., 4$). In the present study the classical choice is adopted by considering an addition of the each state variable contribution as in [22][24]:

$$(s_1, s_2) = \sum_{i=1}^{4} \int_\Omega v_1^i v_2^i dx.$$

This approach allows an important reduction of the number of degrees of freedom in the state system, from $4 \times N_x$ to N_{POD}. Only time-independent boundary conditions are prescribed and the POD has to be calculated on time-centered snapshots ($v^i(x,t) - \overline{v^i(x)}$) because spatial modes can only respect homogeneous boundary conditions. The expansion of each state variable is then:

$$v^i(x,t) \approx \hat{v}^i(x,t) = \overline{v^i(x)} + \sum_{j=1}^{N_{POD}} y_j(t)\Phi_j^i(x), \text{ with } \overline{v^i(x)} = \frac{1}{T}\int_T v^i(x,t)dt. \quad (3)$$

3.2. Projection onto the POD basis and stabilsation strategy

A direct use of the variable expansions (3) in the previously defined compressible system leads to fractional expressions which do not allow trivial Galerkin projection onto the POD basis. An alternative is suggested by [22] to derive a quadratic polynomial ODE system by considering a modified formulation of the state vector $U \rightarrow \tilde{U} = [1/\rho \; u_1 \; u_2 \; p]^t$. The corresponding low-order model is then, for $i = 1, ..., N_{POD}$:

$$\begin{cases} \dot{y}_i = \sum\limits_{j,k=1}^{N_{POD}+1} (a_{ijk} + b_{ijk})\, y_j^+ y_k^+ + \sum\limits_{j=1}^{N_{POD}} c_{ij} y_j + d_i = f_i(c,d,y) \\ y_i(t_0) = (v(x,t_0) - \overline{v(x)}, \Phi_i(x)) \end{cases}$$

with

$$\begin{cases} \Phi^+ = \{\overline{v}, \Phi_1, ..., \Phi_{N_{POD}}\} \\ y^+ = \{1, y_1, ..., y_{N_{POD}}\}. \end{cases}$$

a_{ijk} and b_{ijk} are constant coefficients issued from the projection of the modified advective and diffusive terms of the Navier-Stokes system. The initial conditions of the ODE system are the projections of the modified variable fluctuations onto the reduced basis. This dynamical system represents an approximation of the high-order one which allows important computational savings. However, when the mode truncation is applied on the POD basis, the less energetic modes which contain

dissipative spatial scales, are neglected. This could be an explanation for the inherent instability encountered when integrating POD-Galerkin models. In order to overcome this lack of dissipation, empirical artificial terms are often added in the ODE system [30][8]. Following the approach developed by [10] in the incompressible context, optimal linear and constant coefficients (c_{ij} and d_i) found as solutions of a minimization problem, involving the following objective function, are incorporated in the ROM:

$$J(c,d) = \frac{1}{2}\sum_{i=1}^{N_{POD}}\sum_{j=1}^{N_t}\left(y_i(t_j) - \hat{y}_i(t_j)\right)^2 \text{ with } \hat{y}_i(t_j) = y_i(t_0) + \int_{t_0}^{t_j} f_i(c,d,\hat{y}(t'))dt'. \quad (4)$$

This cost function quantifies at least square sense the prediction error of the ROM with respect to the reference dynamics. The corresponding non-linear optimisation problem is simplified by replacing the predicted dynamics ($\hat{y}(t')$) with the reference ones ($y(t')$) in the Cauchy problem integration, which leads to a linear sytem resolution.

4. Validation results

A high-order simulation is performed over one period of the buffeting mode ($\Delta_t = 0.0437s$) which corresponds to approximately twenty von Kármán periods of the established flow. $2,200$ snapshots ($N_t = 2,200$) are collected regularly in order to build a dataset for the empirical basis extraction. The "snapshot-POD" methodology is applied and N_t spatial POD modes are derived. The eigenvalues associated with these modes (Fig. 2) represent their informational content or "inertia" in the sense of the Principal Component Analysis, as well as the energy contained in the corresponding spatial structures. The dimension reduction consists in retaining only the most energetic modes. The truncation is based on the statistical content conveyed by the first N_{POD} modes:

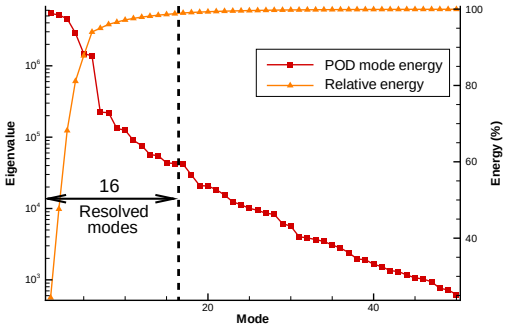

Figure 2. POD mode eigen-spectrum (red squares), global energy reconstruction (orange triangles).

$$I_{N_{POD}} = \left(\sum_{i=1}^{N_{POD}} \lambda_i\right) \Big/ \left(\sum_{i=1}^{N_t} \lambda_i\right).$$

In the present case, $N_{POD} = 16$ modes are taken into account, which represents 99% of the database inertia as shown in Fig. 2. The right hand side of the energy spectrum is neglected when computing the constant coefficients of the POD-Galerkin ODE system, at first. Spatial modes (Fig. 3) are characterised by symmetrical patterns induced by the shape of the transonic flow instabilities. The von Kármán instability is efficiently described by the two first modes whereas the following peer is undoubtedly related to the low frequency buffeting. This fact confirms the relevance of the POD technic in the context of modal analysis. The combination of the two

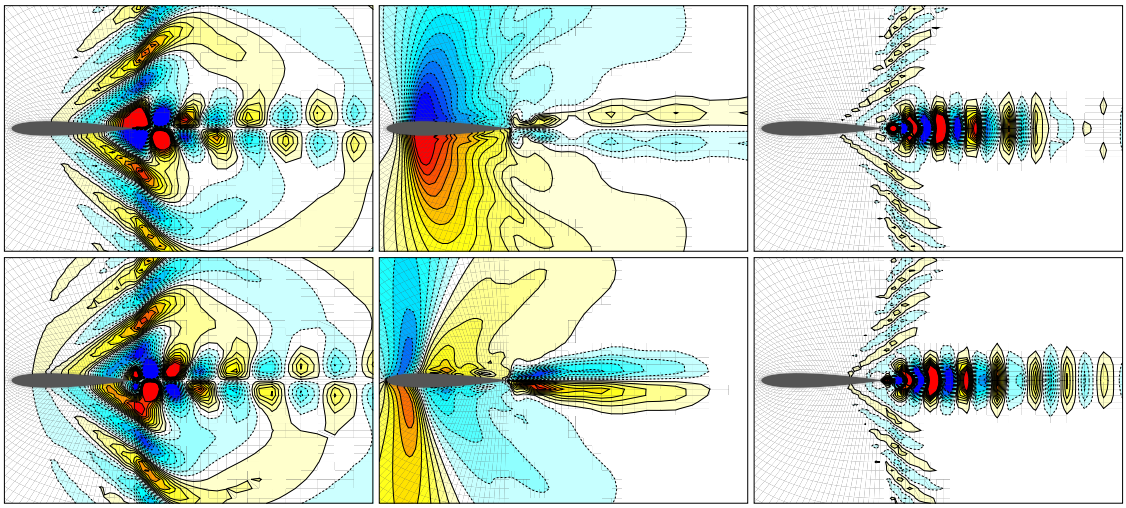

Figure 3. Six first spatial POD modes, $R_e = 10,000$ and $M = 0.8$.

instability modes is emphasised by the first temporal modes represented in Fig. 4: a strong modulation of the von Kármán mode by the low frequency one is observed on the fourth peer.

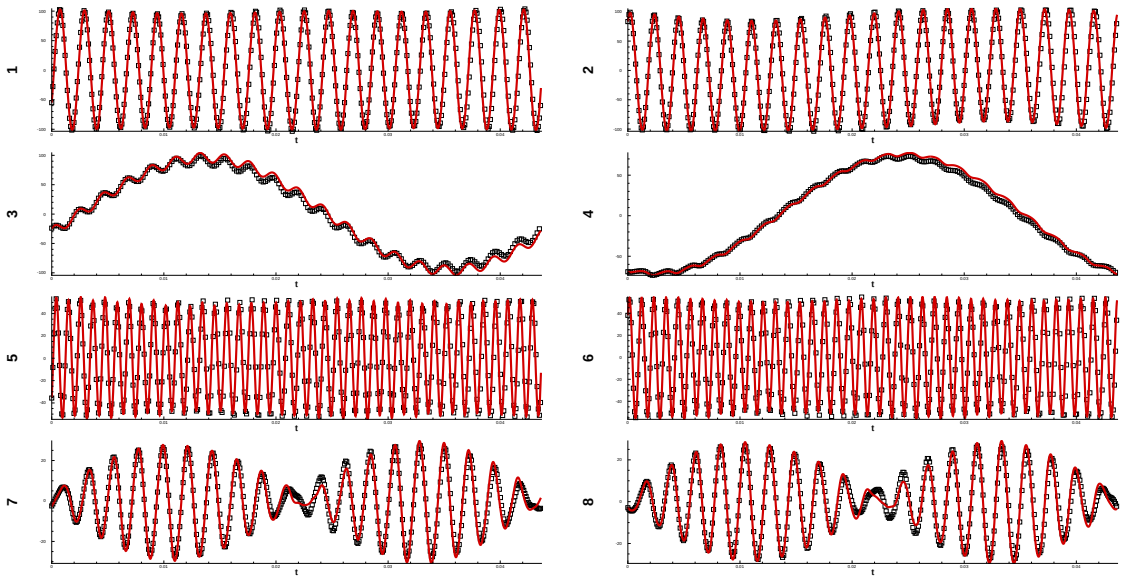

Figure 4. Eight first dynamics over one buffeting period: reference (black squares) and prediction via calibrated ROM (red lines).

The reference temporal modes are issued from the projection of the time-centered database onto the spatial modes. The purpose of the low-order model is to predict these main dynamics. The calibration coefficients are computed on the basis of the minimization of the prediction error (4). These stabilisation terms can be regarded as an "a posteriori" mean to take into account of the truncated part of the POD basis. The integration of the ROM is ensured by a fourth order accuracy Runge-Kutta scheme over the snapshots temporal horizon from the initial condition.

From a numerical point of view, the model reduction induces a considerable gain of computational time, from approximately four hours for the complete Navier-Stokes simulation to 2.9 secondes for the ROM. As shown in Fig. 4 the dynamics are rigorously predicted by the reduced order approach: the signal amplitudes are respected and no phase-lag is observed even for low energy modes as the efficient prediction of the seventh and eighth dynamics proves it. The predicted pressure over a period of buffeting is monitored at two location points: on the airfoil near the trailing edge and in the near wake above the symmetry line (Fig. 5). The prediction by the

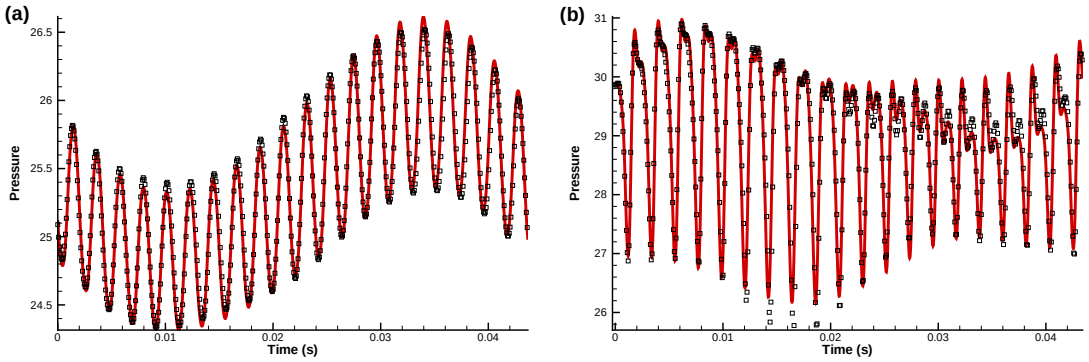

Figure 5. Pressure prediction at two location points, (a) on the airfoil, (b) in the near wake: reference (black squares) and prediction via the calibrated ROM (red lines).

calibrated ROM presents a good match with the reference pressure computed with the high-order Navier-Stokes system.

A global prediction error is defined as follows, at t_i:

$$E(t_i) = \left(\frac{\sum_{j=1}^{4} ||v^j(x,t_i) - \hat{v}^j(x,t_i)||^2}{\sum_{j=1}^{4} ||v^j(x,t_i)||^2} \right)^{1/2},$$

where v^j is the reference and $\hat{v}^j$ the approximation. Over the temporal horizon of the snapshots, the prediction error of the ROM is in the same order of magnitude than the reconstruction error induced by the POD basis truncation (Fig. 6). Moreover, this error remains stable and the weak growth along the period can be explained by a very slight phase-lag which is not significant when considering the whole field prediction after one buffeting period. In Fig. 7 the longitudinal velocity and the pressure fields obtained by high and low-order simulations are represented using the same contour levels. The perfect match observed for both kinematic and thermodynamic variables emphasises the physical relevance of the low-order approach with respect to the complex physical model.

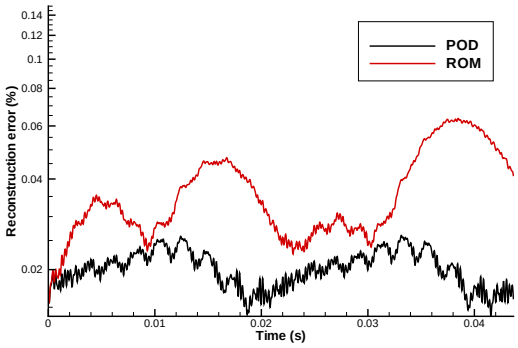

Figure 6. Global reconstruction error of the state variables over one buffeting period: POD filter (black line) and calibrated ROM (red line).

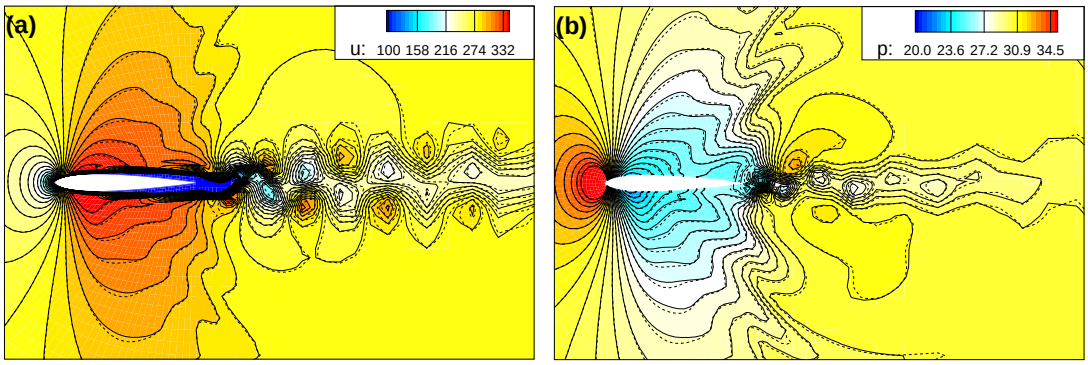

Figure 7. Predicted (a) longitudinal velocity and (b) pressure fields after one buffeting period via Navier-Stokes simulation (plain line) and the present ROM (dahsed lines).

5. Conclusion

In the present study, a low-order model was derived on the basis of the fully compressible Navier-Stokes system. The POD-Galerkin approach was applied on a modified formulation of the high-order system by means of an inner product involving both kinematic and thermodynamic state variable. A statistical criterion based on the reconstruction of the dataset informational content is considered to determine the truncation level. This methodology lead to a simple surrogate model of reduced number of degrees of freedom valid for the prediction of two-dimensional transitional compressible flows around airfoils. The corresponding polynomial ODE system which proved relevant predictive capacities for short term simulations was recalibrated in order to minimize the prediction error with respect to a reference high-order direct simulation, for longer computations. Global dynamics involving the whole state variables were integrated in time and the physical reliability of the present low-dimensional approach was examined on a transonic test-case characterised by an unsteadiness induced by compressibility effects. The interaction between the von Kármán instability and the lower frequency buffeting mode is efficiently predicted by the ROM as the comparison with the Navier-Stokes simulation results proves it.

Acknowledgments

The calculations were performed at the Centre Informatique National de l'Enseignement Supérieur (CINES), the Institut du Développement et des Ressources en Informatique Scientifique (IDRIS) and the Centre Interuniversitaire de Calcul de Toulouse (CICT). The first author was financially supported by the Centre National de la Recherche Scientifique (CNRS) and the Délégation Générale pour l'Armement (DGA) which are gratefully acknowledged.

References

[1] G. BERKOOZ, P. HOLMES and J.L. LUMLEY. *The proper orthogonal decomposition in the analysis of turbulent flows.* Ann. Rev. Fluid Mech., 25:539-575, 1993.

[2] K. KARHUNEN. *Zur spektraltheorie stochasticher prozesse.* Ann. Acad. Sci. Fennicae, A1, 34, 1946.

[3] J. DELVILLE, L.S. UKEILEY, L. CORDIER, J.P. BONNET and M.N. GLAUSER. *Examination of large-scale structures in a turbulent plane mixing layer. Part 1. Proper orthogonal decomposition.* J. Fluid Mech., 391:91-122, 1999.

[4] A. DEANE, I. KEVREKIDIS, G.E. KARNIADAKIS and S. ORSZAG. *Low-dimensional models for complex geometry flows: application to grooved channels and circular cylinders.* Phys. Fluids A, 3:2337-2354, 1991.

[5] W. CAZEMIER, R.W.C.P. VERSTAPPEN and A.E.P. VELDMAN. *Proper orthogonal decomposition and low-dimensional models for driven cavity flows.* Phys. Fluids, 10(7):1685-1699, 1998.

[6] X. MA and G.E. KARNIADAKIS. *A low-dimensional model for simulating three-dimensional cylinder flow.* J. Fluid Mech., 458:181-190, 2002.

[7] M. BUFFONI, S. CAMARRI, A. IOLLO and M.V. SALVETTI. *Low-dimensional modelling of a confined three-dimensional wake flow.* J. Fluid Mech., 569:141-150, 2006.

[8] S. SIRISUP and G.E. KARNIADAKIS. *A spectral viscosity method for correcting the long-term behavior of POD models.* J. Computat. Phys., 194:92-116, 2004.

[9] B. GALLETTI, C.H. BRUNEAU, L. ZANNETTI and A. IOLLO. *Low-order modelling of laminar flow regimes past a confined square cylinder.* J. Fluid Mech., 503:161-170, 2004.

[10] M. COUPLET, C. BASDEVANT and P. SAGAUT. *Calibrated reduced-order POD-Galerkin system for fluid flow modelling.* J. Computat. Phys., 207:192-220, 2005.

[11] B.R. NOACK, K. AFANASIEV, M. MORZYNSKI, G. TADMOR and F. THIELE. *A hierarchy of low-dimensional models for the transient and post-transient cylinder wake.* J. Fluid Mech., 497:335-363, 2003.

[12] W.R. GRAHAM, J. PERAIRE and K.Y. TANG. *Optimal control of vortex shedding using low-order models.* Int. J. Numer. Meth. Engng., 44:973-990, 1999.

[13] K. KUNISH and S. VOLKWEIN. *Galerkin proper orthogonal decomposition methods for parabolic problems.* Numerische Mathematik, 90:117-148, 2001.

[14] E. ARIAN, M. FAHL and E.W. SACHS. *Trust-Region Proper Orthogonal Decomposition for Flow Control.* NASA/CR, 210124, 2000.

[15] M. BERGMANN, L. CORDIER and J.P. BRANCHER. *Optimal rotary control of the cylinder wake using POD Reduced Order Model.* Phys. Fluids, 17(9):1-21, 2005.

[16] T. BUI-THANH, M. DAMODARAN and K. WILLCOX. *Proper Orthogonal Decomposition Extensions For Parametric Applications in Transonic Aerodynamics.* AIAA paper, 4213, 2003.

[17] M. MORZYNSKI, W. STANKIEWICZ, B.R. NOACK, F. THIELE, R. KING and G. TADMOR. *Generalized Mean-Field Model for Flow Control Using a Continuous Mode Interpolation.* AIAA paper, 3488, 2006.

[18] D.J. LUCIA, P.S. BERAN and W.A. SILVA. *Reduced-order modeling: new approaches for computational physic.* Prog. in Aero. Sci., 40:51-117, 2004.

[19] F. LI, G. TADMOR, B.R. NOACK, A. BANASZUK and P.G. MEHTA. *A Reduced Order Model for the Reacting Flameholder.* AIAA paper, 3487, 2006.

[20] D.J. LUCIA and P.S. BERAN. *Projection methods for reduced order models of compressible flows.* J. Computat. Phys., 188:252-280, 2003.

[21] C.W. ROWLEY, T. COLONIUS and R.M. MURRAY. *Model reduction for compressible flows using POD and Galerkin projection.* Phys. D, 189:115-129, 2004.

[22] G. VIGO, A. DERVIEUX, M. MALLET, M. RAVACHOL and B. STOUFFLET. *Extension of methods based on the proper orthogonal decomposition to the simulation of unsteady compressible Navier-Stokes flows.* Computational Fluid Dynamics'98, Proc. of the Fourth ECCOMAS Conf., 648-653, Wiley, 1998.

[23] G. VIGO. *The Extension of P.O.D. to Complex System with Non-Homogenous Boundary Conditions, Application to a Turbulent Pulsed Jet.* INRIA RR, 3945, 2000.

[24] A. IOLLO, S. LANTERI and J.A. DESIDERI. *Stability properties of POD-Galerkin approximations for the compressible Navier-Stokes equations.* Theor. Comput. Fluid Dyn., 13:377-396, 2000.

[25] A.BOUHADJI and M. BRAZA. *Organised modes and shock-vortex interaction in unsteady viscous transonic flows around an aerofoil, Part I: Mach number effect.* Comp. Flui., 32:1233-1260, 2003.

[26] A.BOUHADJI and M. BRAZA. *Organised modes and shock-vortex interaction in unsteady viscous transonic flows around an aerofoil, Part II: Reynolds number effect.* Comp. Flui., 32:1261-1281, 2003.

[27] H.L. SEEGMILLER, J.G. MARVIN and L.L. LEVY. *Steady and Unsteady Transonic Flow.* AIAA J., 16(12):1262-1270, 1978.

[28] O. RODRIGUEZ. *The circular cylinder in subsonic and transonic flow.* AIAA J., 22(12):1713-1718, 1984.

[29] L. SIROVITCH. *Turbulence and the dynamics of coherent structures, Part I-III.* Quart. Appl. Math., 45(3):561-590, 1987.

[30] N. AUBRY, P. HOLMES, J. LUMLEY and E.STONE. *The dynamics of coherent structures in the wall region of a turbulent boundary layer.* J. Fluid Mech., 192:115-173, 1988.